ORIGINAL PAPER

Tribological Behaviour of Ti6Al4V Alloy: An Application in Small Joint Implants

Lukáš Odehnal[1] · Matúš Ranuša[1] · Martin Vrbka[1] · Ivan Křupka[1] · Martin Hartl[1]

Abstract

The presented study deals with the analysis of the tribological behaviour of the Ti6Al4V alloy manufactured conventionally. The study aimed to verify whether the titanium alloy is suitable for use as a contact material in small joint implants, as additive manufacturing of this alloy can in the future provide certain benefits, such as individualization and simplification of the implant construction, or controlled porosity. The tested pair consisted of a pin and a glass plate lubricated with model synovial fluid. The contact area was observed with colorimetric interferometry. Alongside film thickness, friction, and wear scars were measured. From the designed experimental conditions, the titanium alloy was not able to create a sufficiently thick lubrication film to overcome its surface roughness and damage to contact surfaces occurred. Friction was comparable for all the tested configurations. The application of conventionally manufactured titanium alloy as a contact surface in small joint implants seems to not be suitable since its performance fell short when compared to conventional cobaltous alloy. Nevertheless, there are various alternative methods available, such as unconventional manufacturing, polishing, surface texturing, and coating.

✉ Lukáš Odehnal
  Lukas.Odehnal@vut.cz

1 Department of Tribology, Faculty of Mechanical
   Engineering, Brno University of Technology, Technická
   2896/2, 616 69 Brno, Czech Republic

Graphical Abstract
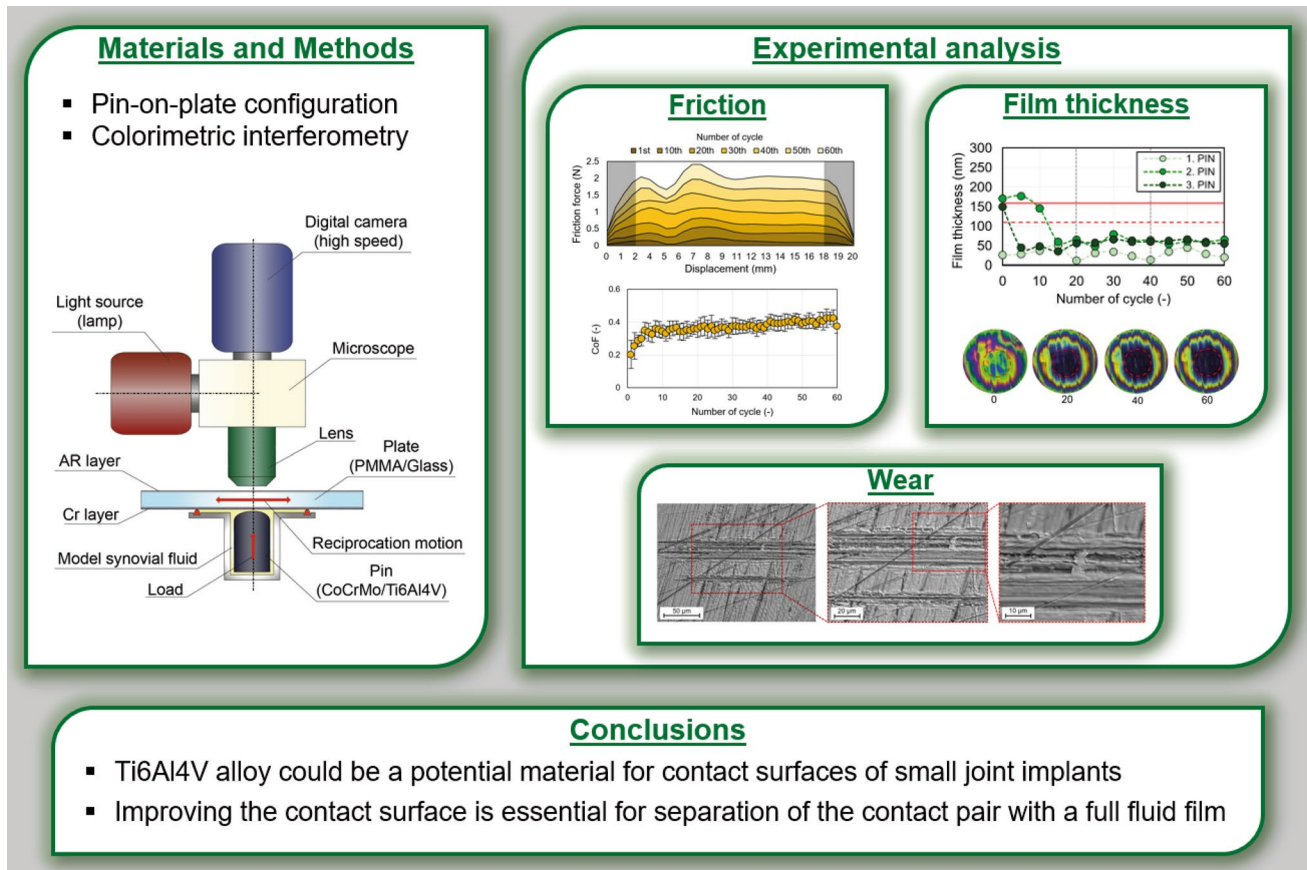
1 Introduction

Interventions, especially the replacements of human joints, have become a necessity for today's population. The number of all joint replacements applied to the human body is rising every year. In the human body, there are various kinds of joints, and their full functionality is necessary for everyday life, for example, small joints, such as the big toe's first metatarsophalangeal joint (first MTP joint). This joint is responsible for a person's stability and is the most stressed joint in the foot during normal movement activities. Based on the study by Korim et al. [1] which reviewed the conducted arthrodesis, hallux valgus and hallux rigidus are the most frequent diseases affecting the first MTP joint, accounting for 36.6% and 34% of the cases, respectively. Recently, mainly hallux valgus has been discussed, as many middle-aged women suffer from this deformity because it is closely associated with wearing tight shoes or high heels. There are two main approaches to treating these deformities. The first, which is mainly invasive, is arthrodesis (fusion).

This is a definitive and irreversible operation in which the affected joint is immobilized by fusing the bones together. The second option is joint arthroplasty. With this method, the joint motion can be preserved and this intervention does not affect the gait pattern [2]. Based on the statistics from Germany [3], between 2008 and 2017, only a few of the first MTP joint arthroplasties were made compared to arthrodesis, although it may have certain benefits. On the other hand, the first MTP joint replacements are not as reliable as arthrodesis these days. One of the most common types of total arthroplasty for the first MTP joint is ToeFit-Plus® [2]. Titchener et al. [4] reported a revision rate of 24% at an average of 33 months post-operatively for this implant, while the majority of revisions were caused by frank loosening or progressive lucency, mainly on the phalangeal side.

The first MTP joint replacements evolved in shape or used materials in the past [5]. During these days, the most common type is a metal-on-polyethylene total MTP replacement. These replacements consist of two stems from titanium alloy with porous structures, a CoCrMo metatarsal head, and

UHMWPE phalangeal plateau. Lately, additive manufacturing (AM) has become more frequent in all production areas, and this method is also suitable for joint replacements as the AM might bring benefits in the production of personalized metal-on-metal (MoM) small joint implants [6]. The most common method for producing artificial joints is selective laser melting (SLM) [7]. In such manufacturing, Ti6Al4V is more suitable than common CoCrMo alloy which is the most common contact surface in joint replacements these days [8]. The titanium alloy has excellent biocompatibility, good corrosion resistance, and high strength ratio [9]. Moreover, this alloy fabricated with a porous structure has comparable mechanical properties to a natural bone and can improve ingrowth of the stems and increases bone-implant stability [10]. To ensure the applicability of Ti alloy, the material must be subjected to detailed testing and compared with conventional Co alloy based on their performances.

To bring the experimental conditions close to reality, boundary conditions, such as kinematics and load, have to be defined. The kinematics of the first MTP joint was described by Durrant et al. [11]. The model provided knowledge about the joint movements and described their variance between the individual subjects. The loading of the joint, or the contact pressure, was examined by Flavin et al. [12] and Al-Munajjed et al. [13]. The main feature ensuring the proper behaviour of the replacement in the human body is the ability to form a sufficiently thick lubrication film that can separate interacting parts of the replacement in order to reduce the generation of wear particles.

The formation and thickness of the lubrication film can be influenced by various parameters. Myant et al. [14] demonstrated the impact of contact pressure, where its increase resulted in a decrease of lubrication film thickness. Kinematics, respectively the relative speed and slide-to-roll ratio (SRR) was described by Nečas et al. [15], who showed that the relative speed works differently for various SRR, i.e., the increase in relative speed for SRR 0 led to an increase in film thickness; on the other hand, for SRR 1.5, it led to a decrease in film thickness. Another factor potentially influencing the behaviour may be connected to contact surfaces, as human joints are tested with synovial fluid (SF) consisting of proteins with the ability to adsorb on the contact surfaces and its presence can affect the overall behaviour [16] of the system. The ability to form a stable and sufficiently thick lubrication film is usually connected to the number of proteins in the contact area. Nečas et al. [17] presented that the behaviour of lubrication film thickness is dependent on the composition of SF and tried to connect the behaviour of individual constituents, such as albumin and γ-globulin, to the lubrication film thickness. It was found that the trends of albumin and lubrication film thickness were comparable, while the γ-globulin development was observed only on a small scale [15]. Therefore, it appears that the main role of

forming the lubrication film lies in albumin, while its presence and maintenance in the contact area might be affected by other constituents [18, 19]. The study made by Ranuša et al. [20] showed differences in the behaviour of samples with differences in surface topography. The tested Ti alloy had significantly worse surface roughness compared to Co alloy, resulting in the presence of a larger amount of proteins in the contact area. The well-formed and stable lubrication film is closely connected to other observed parameters, such as friction and wear, while these two parameters are closely related to good functionality and the lifetime of the replacement.

In the case of load, the increase of normal force leads to a decrease in friction [21, 22]. On the other hand, while lower friction occurs in higher load conditions, findings by Gao et al. [23] showed that the higher load contact is more likely to produce a higher rate of wear particles; therefore, lower friction does not always mean a lower wear rate. The studies dealing with the lubricant concentration [24–26] similarly showed that friction increases with an increasing number of proteins in the lubricant. When comparing the Co and Ti alloys according to the coefficient of friction (CoF), the values are not so different [27] On the other hand, when comparing the generation of wear particles, the titanium alloy is worse, while the released particles were approximately twice as high as for CoCrMo [28]. These findings could mean that the titanium alloy is incompatible with the use in the joint implants for contact surfaces, as the excessive number of released particles is undesirable for the patient's health [29]. Nevertheless, the benefits coming with additive manufacturing and simplifying the implant shape construction predetermine that the use of this alloy could find its application.

Based on the performed research and the knowledge gained in the past in this area of interest, further and complementary research seems more than needed since a better understanding of the given phenomena can lead to an increase in the lifespan and functionality of the implant, which are currently a big problem, as the revision operations rate is still too high for this joint [4]. To obtain such research that can reveal the behaviour in the contact area, the problem has to be examined at its roots. The main question posed in this publication was *"What are the main differences in the tribological behaviour of conventionally manufactured CoCrMo and Ti6Al4V alloys in the simulated small joint implant (first MTP joint)?"* and the sub-question: *"Is the Ti6Al4V alloy suitable for further investigation as a potential material for human joints?"* To answer these questions, the research is supplemented with the development of lubrication film thickness, an analysis of friction, and an analysis of contact pair roughness, or its wear scars. Combining these observed aspects should provide the necessary insight into the issue and show whether it makes sense to conduct further research on Ti6Al4V alloys as possibilities for contact

surfaces in small human joints, where additive manufacturing might find its application.

2 Materials and Methods

2.1 Experimental Apparatus

The experiments were performed on the universal tribometer [20, 30], providing reciprocal movement in a pin-on-plate configuration with a stable sample (pin) and a moving plate (glass). The experimental apparatus is shown in Fig. 1. The tribometer construction enables the use of optical methods to observe the contact area and measurement of the friction simultaneously. As the main goal of the study was to describe the lubrication mechanism, colorimetric interferometry [31] was used to observe the contact area to obtain information on the film thickness and its development.

2.2 Contact Pair and Lubricant

The contact pair consisted of a pin made from alloys used in implantology: CoCrMo (ASTM-F75) or Ti6Al4V (ISO

Fig. 1 Scheme of the experimental apparatus

5832-3). The implant manufacturer [32] produced the test pins using a certified process involving cold drawing, followed by machining to a 15 mm radius, and polishing to a roughness of Ra = 0.01 ± 0.005 μm for CoCrMo, and Ra = 0.04 ± 0.01 μm for Ti6Al4V as the conventional machining for joint implants allowed for the used materials. The finishing process followed the certified method, which showed that it was not possible to bring the surface roughness of Ti6Al4V alloy closer to the one obtained for CoCrMo alloy. The second articulating part was a plate made from B270 glass, as one transparent part was necessary for observations using colorimetric interferometry. To enhance the observation conditions, the plate was on the contact surface coated with the Chromium layer (reflectivity of 25%). The other side of the plate was covered with an antireflective layer. The use of counterpart made from glass shows that the observed simulated joint more likely corresponds to the metal-on-metal joint implant type, as the material characteristics are closer to each other than for the metal-on-polymer type. The material characteristics of contact bodies are shown in Table 1.

The presented study used the model SF as the testing lubricant. The model SF was synthetically prepared based on the samples extracted from patients with arthroplasty [33]. The final composition of the model SF was made by diluting the required number of constituents in phosphate-buffered saline (PBS). The concentration of diluted components, respecting the properties of SF for patients after arthroplasty, is as follows: albumin (26.3 mg/ml), γ-globulin (8.2 mg/ml), hyaluronic acid (0.82 mg/ml), and phospholipids (0.35 mg/ml).

2.3 Loading and Kinematic Conditions of Experiments

As there is no available ISO standard for testing of small joint implants, especially the first MTP joint investigated in this study, the loading and kinematic conditions had to be determined based on the analytic models or ISO standards used for testing of total knee replacement (TKR) [34] or total hip replacements (THR) [35]. Durrant et al. [11] presented a model where the initial metatarsal declination angle is 15°, and the terminal declination angle is approximately 80°; these angles can vary for different subjects. Using a
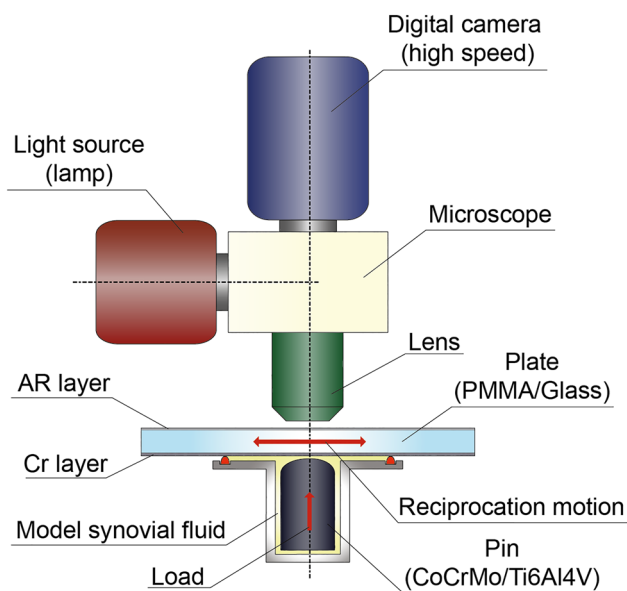
Table 1 Material characteristics, loading, and the resulting contact area based on the Hertz theory

Material	Young's modulus	Poisson's ratio	Applied load	Contact pressure	Calculated contact area
CoCrMo	241 GPa	0.29	0.5 N	105.5 MPa	0.095 mm
Ti6Al4V	114 GPa	0.34	0.73 N	105.5 MPa	0.115 mm
Glass B270	71 GPa	0.22			

typical radius of total replacements for this joint, the contact path was calculated for ~ 12 mm. Nevertheless, the 20 mm stroke was used in the experiments due to dead ends occurring in the testing cycle as the measuring of friction and observing the contact area requires a sufficiently long stroke with stable normal load and speed stabilization. The tested speeds were chosen according to the speeds that may appear in the 1. MTP joint during the gait cycle based on the sagittal plane kinematics presented by Allan et al. [36]. Based on the development of the declination angle, the recalculation of peripheral speed was made. Considering that the duration of the cycle is one second [34, 35] and the typical radius of rotation for the 1. MTP joint is about 13 mm [37, 38]; the recalculation showed that for the most of the cycle, the speed is very low (approx. 1–6 mm/s). The considerable speeds occur between 40 and 65% of the cycle, varying from 7 to 65 mm/s. Two speeds, 20 mm/s and 40 mm/s, were selected from this range for the experiments. The expected contact pressure is in the 1. MTP joint highly influenced by high conformity of the implant's parts, where both curvature radiuses are 10 mm. This results in contact pressure at about 7–8 MPa [12]. When transformed to the experimental conditions (pin-on-plate), this contact pressure (~ 7.9 MPa) is obtained for the material combination of CoCrMo and UHMWPE by applying 0.5 N. In order to maintain the recalculated contact force of 0.5 N on the material combination used in experiments (CoCrMo on Glass), the resulting contact pressure was 105.5 MPa. To compare the behaviour of two tested materials (CoCrMo and Ti6Al4V), the contact pressure was unified in this study. The resulting contact forces applied on two tested configurations after recalculation based on the contact Hertz theory are as follows: 0.5 N (CoCrMo/Glass) and 0.73 (Ti6Al4V/Glass). The load was monitored and controlled during the experiments to ensure no more than ± 5% deviation from the desired value.

2.4 Experimental Setup and Evaluation of the Results

The experiments were designed to observe the behaviour of lubrication film thickness in short terms. The experiment was divided into three parts. After each part, the contact pair was unloaded to depict the relief of the joint. Each partial experiment consisted of 20 cycles, which gives the number of 60 cycles for the whole experiment, composed of two unloading stages. Each configuration was tested on three different contact pairs to achieve sufficient repeatability. The presented results were evaluated from the observation of contact in only one direction (marked as "Evaluated area" in Fig. 2A). This area is also cropped off the first and last 2 mm of the deflection; as in these parts (dead ends) of the cycle, the relative speed was not constant and it was not marked as relevant to the results. Continuous development of both
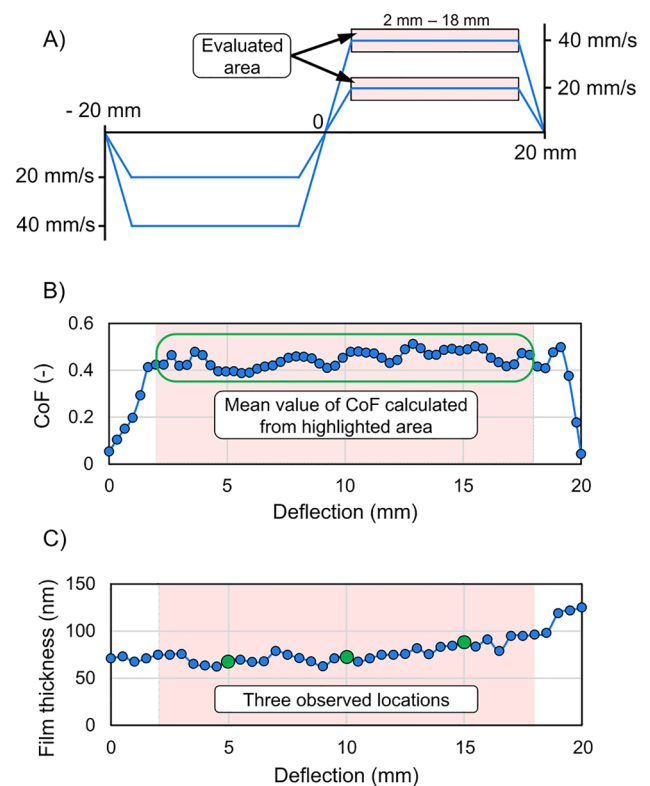

Fig. 2 Scheme for the evaluation of the results: **A** relative speeds with a marked area of evaluation; **B** evaluation of CoF; **C** evaluation of lubrication film thickness

CoF and lubrication film thickness was recorded during the experiment (see Fig. 2B, C). For CoF, the whole marked area – green oval (see Fig. 2B) is represented in the results by the average value for each cycle. While observing the lubrication film thickness and its development over time, it was found out that the thickness was dependent on the observed point of the cycle. In light of this finding, three points were selected and observed to describe possible inconsistencies during the cycle. These points are marked green in Fig. 2C.

3 Results

3.1 Analysis of Surface Roughness Before the Experiment

A roughness analysis of the samples was carried out to define the boundaries of lubrication film thickness, i.e., a separation of the contact surfaces with a certain probability. A sufficiently close zone adjacent to the contact area was selected for this observation. The zone was based on the expected size of the calculated contact area, which was doubled in cases where the contact area did not appear on the expected canopy. The surface roughness distribution

(its irregularities) of both examined alloys was Gaussian. Two borders were determined, the first representing a 95% probability of separation of contact pairs and the second a 99% probability. The values were established based on the measurements (see Table 2) to 35 nm (CoCrMo) and 110 nm (Ti6Al4V) for a probability of 95%, or to 45 nm (CoCrMo), and 160 nm (Ti6Al4V) for a probability of 99%. These borders are represented in the results graphs as red dashed, or solid lines.

3.2 Lubrication Film Thickness

For the lubrication film thickness, the experiments with an entrainment speed of 20 mm/s (see Fig. 3) showed similar results in case of reaching a sufficiently thick film layer for both of the materials, and the separation of contact pairs did not occur (except for the first few cycles for 2. PIN made from Ti alloy). The measured thickness was generally higher for the Ti alloy (e.g. point at 10 mm deflection at 30th cycle: ~ 15 nm for CoCrMo and ~ 55 nm for Ti6Al4V). Nevertheless, due to its worse surface roughness, it was not sufficiently high as the thickness did not reach either of the shown boundaries (red dashed or solid line).

On the other hand, the experiments with an entrainment speed of 40 mm/s showed different results for each material (see Fig. 4). While using the CoCrMo alloy, the contact pairs were separated for almost the whole experiment (except for the first few cycles for 1. PIN). On the contrary, while the Ti6Al4V alloy was used, the film thickness showed quite similar behaviour as at a lower speed and it did not reach sufficient values to separate the contact pair completely (except for the first few cycles for 2. and 3. PIN).

3.3 Wear Scars after Experiments

The findings regarding the lubrication film thickness of tested samples correspond with the roughness measurements (wear scar analysis) after experiments, where a combination of CoCrMo and glass at 40 mm/s showed no signs of wear.

Table 2 Probability of full film lubrication based on contact pair roughness

Material	Sample	95% Probability of separated contact pairs	99% Probability of separated contact pairs
CoCrMo	PIN 1	30 nm	41 nm
	PIN 2	35 nm	47 nm
	PIN 3	34 nm	48 nm
Ti6Al4V	PIN 1	102 nm	166 nm
	PIN 2	113 nm	182 nm
	PIN 3	100 nm	128 nm

Overall, the wear scars on the tested samples differ for each material and relative speed applied (see Fig. 5 and Table 3).

The CoCrMo samples are most likely to create a regular oval wear area oriented with a longer axis in the direction of the movement (Fig. 5A). On the other hand, the Ti6Al4V pins did not create such an oval wear area, but these samples were characterized by the formation of separated grooves that were considerably deeper and also longer in the direction of the movement (Fig. 5B). Table 3 shows the characteristics of the wear scars for all tested samples. Significant differences were observed for Ti alloy pins at 20 mm/s where 1. PIN showed similar wear scars as Co pins (oval area) and 2. PIN had no scars at all.

The typical wear scars for each material are illustrated more precisely in Fig. 6. The wear mechanism of Ti6Al4V and CoCrMo alloys differs, as observed in the images. The images of Ti6Al4V show a non-uniform wear pattern accompanied by the creation of deeper separate grooves, while the wear area of the CoCrMo sample is characterized by the creation of regular oval wear areas without irregularities. The images depict the abrasion for both materials, but the release of Ti6Al4V wear particles caused the three-body abrasion.

3.4 Coefficient of Friction

Figure 7 shows the evolution of CoF for all tested configurations. The yellow dots, representing the average value of CoF for three samples are in the graphs supplemented with standard deviation (SD). All configurations showed a similar behaviour, with CoF settled down at values around 0.4 after an initial increase. The rehydration stages after 20 or 40 cycles (marked with vertical black dashed lines) did not significantly affect the behaviour of CoF at the tested speeds of 20 mm/s. On the other hand, when the relative speed of 40 mm/s was applied, a slight decrease of CoF can be seen after the rehydration stages for Ti6Al4V and a much greater decrease for CoCrMo. Nevertheless, the decrease lasted only one cycle and then the friction returned to the expected value. The values of CoF for CoCrMo at 40 mm/s (the only configuration that reached the selected boundaries for separated contact pairs) were the most inconsistent with the highest SD (see Fig. 7D).

The development of friction was supplemented with stacked graphs of friction force evolution throughout the experiments for each configuration (see Fig. 8).

The friction force values were evaluated using the methodology outlined in Fig. 2A as averages of three repeated experiments. Grey stripes indicate the beginning and end of each cycle, representing parts of the cycle, where the relative speed was unstable. Each material displayed a unique stacked pattern of the evolution due to the application of different loading forces. The development in each cycle
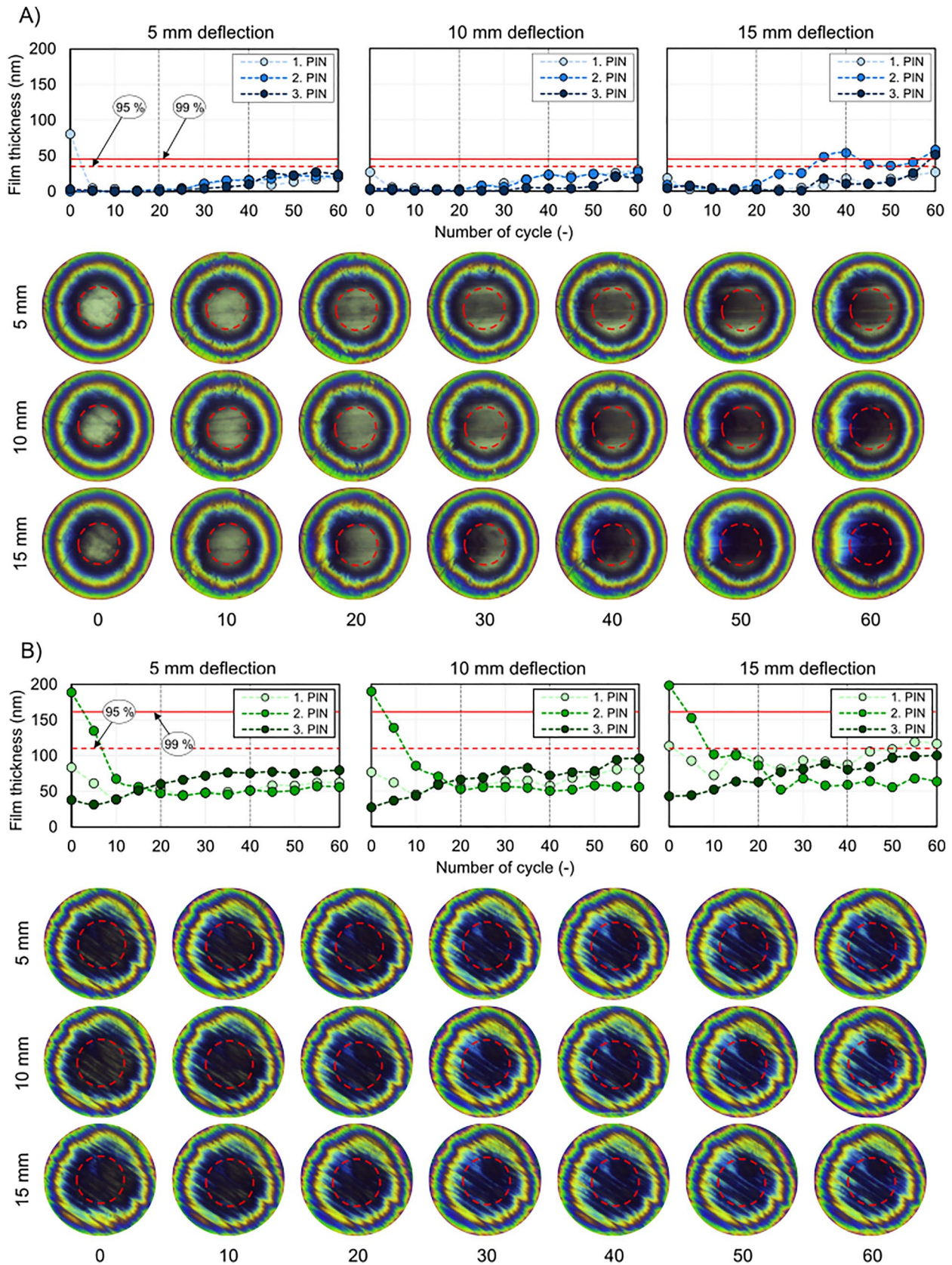
Fig. 3 Development of film thickness at 20 mm/s for **A** CoCrMo and **B** Ti6Al4V. Interferograms with marked contact areas correspond to 3. PIN for each configuration (the inlet zone is on the left side)
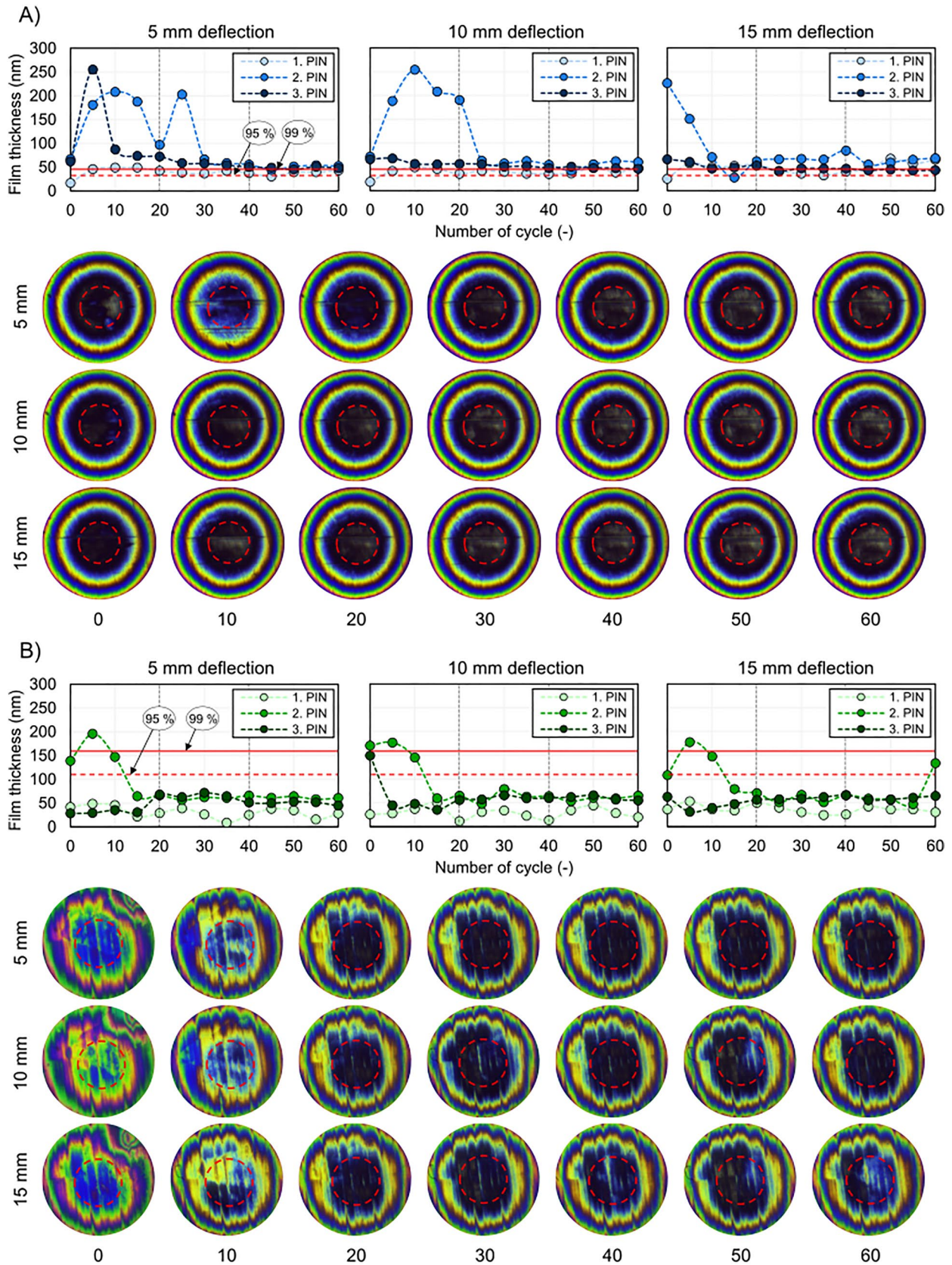
Fig. 4 Development of film thickness at 40 mm/s for **A** CoCrMo and **B** Ti6Al4V. Interferograms with marked contact areas correspond to 3. PIN (CoCrMo) and 2.PIN (Ti6Al4V) (the inlet zone is on the left side)
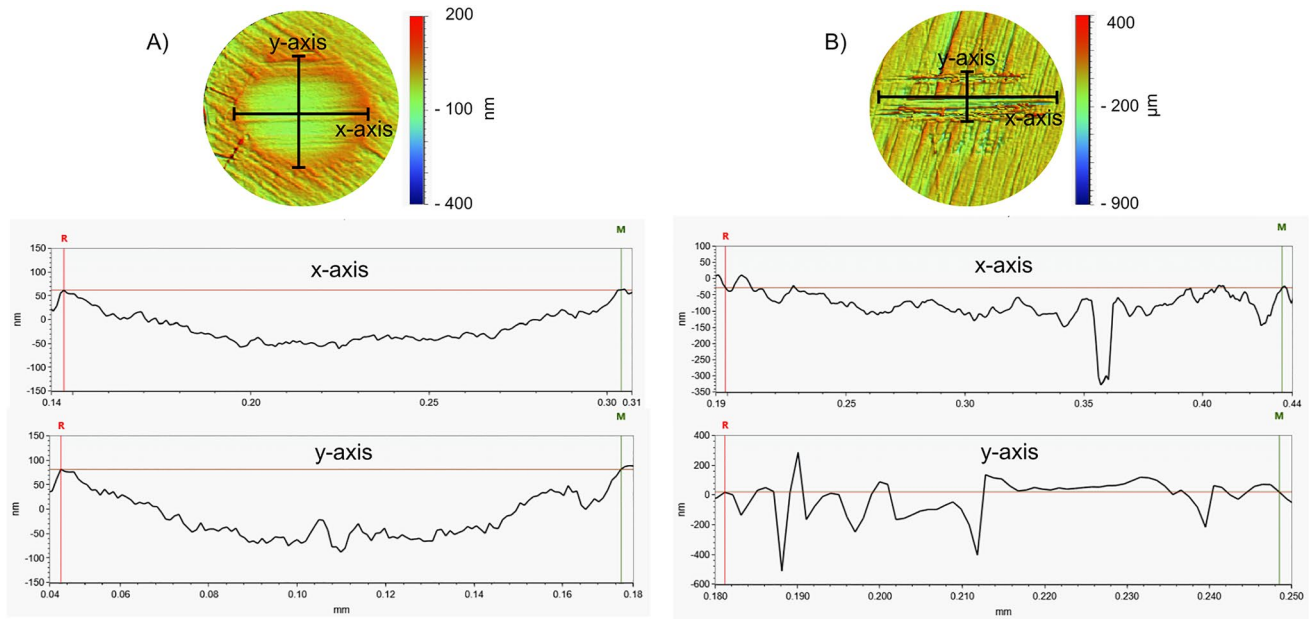
Fig. 5 Wear scars on **A** CoCrMo samples, and **B** Ti6Al4V samples. Graphs represent the profile cuts of PIN 1 of each material with marked borders (red and green lines), corresponding to surface pictures of wear areas

Table 3 Wear scars on tested samples

Tested conditions	Sample	x-axis width	y-axis width	Central depth	Tested conditions	Sample	x-axis width	y-axis width	Central depth
CoCrMo Glass 20 mm/s	PIN 1	157 µm	124 µm	86 nm	Ti6Al4V Glass 20 mm/s	PIN 1*	168 µm	123 µm	127 nm
	PIN 2	139 µm	120 µm	92 nm		PIN 2	Non-visible signs of wear		
	PIN 3	126 µm	86 µm	81 nm		PIN 3	139 µm	87 µm	203 nm
CoCrMo Glass 40 mm/s	PIN 1	Non-visible signs of wear			Ti6Al4V Glass 40 mm/s	PIN 1	255 µm	154 µm	583 nm
	PIN 2	Non-visible signs of wear				PIN 2	196 µm	65 µm	437 nm
	PIN 3	Non-visible signs of wear				PIN 3	298 µm	131 µm	984 nm

*The wear scar of the Pin was similar to the ones in CoCrMo/Glass configuration

remained quite stable during the entire experiment after the initial rise due to the increase in relative speed for all configurations except for the Ti6Al4V at 40 mm/s, where an additional lower peak occurred at around 5 mm, and the upper peak at around 7 mm of displacement.

4 Discussion General Discussion

The presented study focused on comparing and describing the tribological behaviour in the contact area of two materials suitable for human joint implants, a conventional CoCrMo alloy, and a 3D printing-friendly Ti6Al4V alloy. The experiments were designed to provide a general overview of these two conventionally manufactured materials. Three tribological parameters were measured or observed: lubrication film thickness, friction coefficient, and wear scars on the tested pins. The kinematics and load used in the experiments on the reciprocal tribometer with pin-on-plate configuration [30] were designed based on the literature [11–13] or ISO standards [34, 35], while the deflection in one direction was set at 20 mm. To obtain a frequency of 0.5 Hz and 1 Hz, the applied entrainment speed was 20 mm/s and 40 mm/s, respectively. The load was set to 0.5 N for CoCrMo alloy and 0.73 N for Ti6Al4V, as it was recalculated using the Hertz contact theory based on similar contact pressures.

The experiments showed that it is difficult to create a sufficiently thick lubrication film layer under the experimental conditions designed, as the height of the lubricant did not reach values sufficient to overcome the average roughness of the contact pair (see Figs. 3 and 4). This is accompanied by the formation of wear scars that are undesirable in human joints (see Fig. 5 and Table 3), as
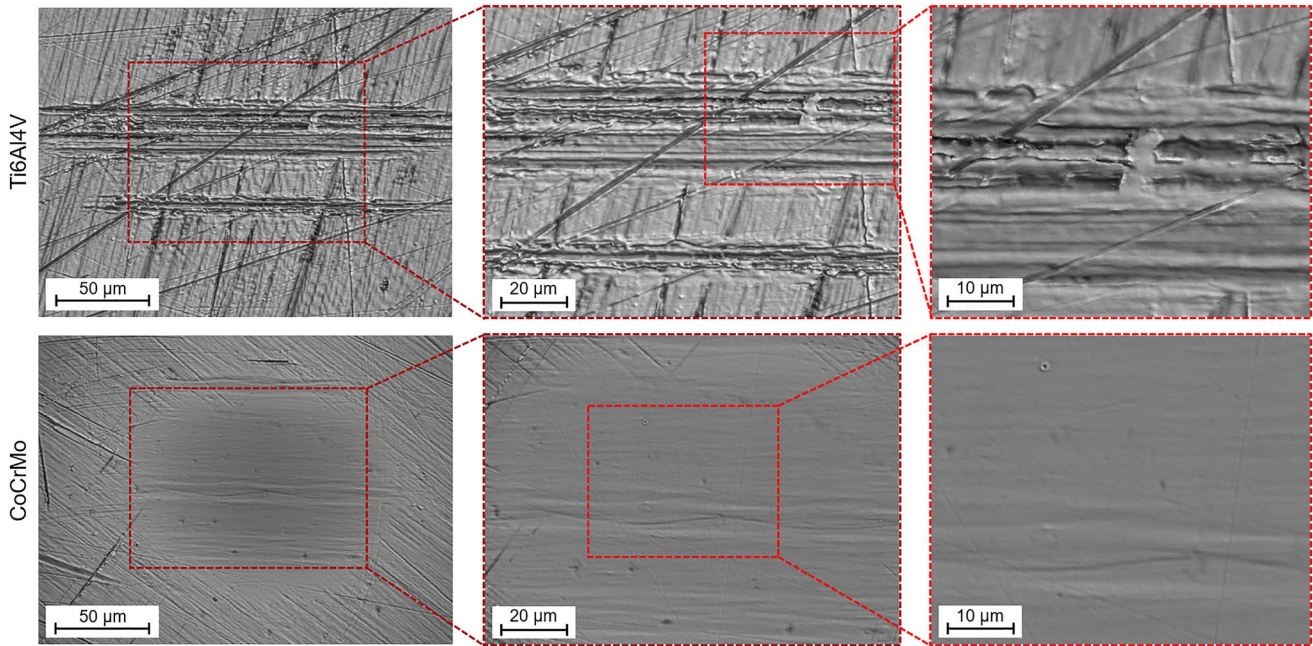
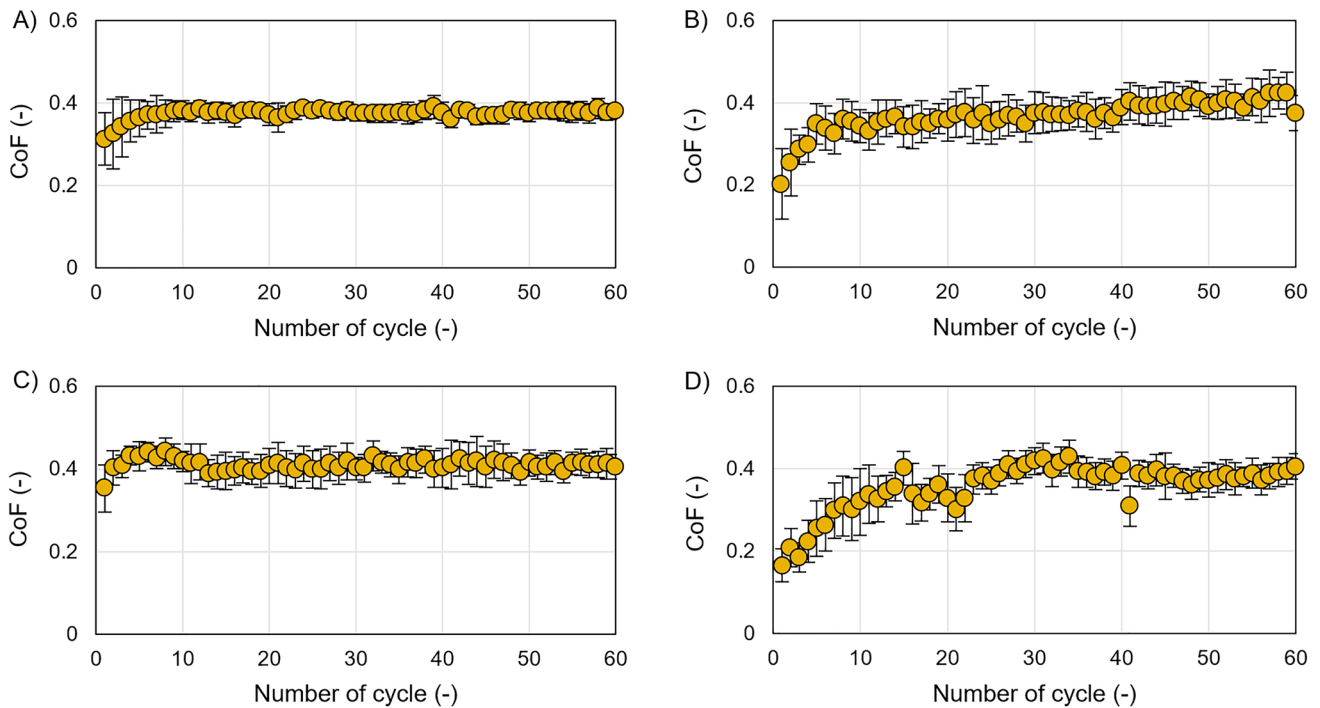**Fig. 6** Comparison of wear scars for Ti6Al4V and CoCrMo alloy at 20 mm/s

Fig. 7 Development of CoF for Ti6Al4V **A** 20 mm/s, **B** 40 mm/s and CoCrMo **C** 20 mm/s, **D** 40 mm/s

they are associated with the release of wear particles into the human body. The only difference was observed for the CoCrMo alloy at 40 mm/s, where the lubrication film thickness reached the limit of 95% probability of contact separation and also reached the 99% probability in some cycles. The formation of a sufficiently thick film layer is accompanied by non-visible signs of wear on these pins (see Table 3). Throughout all experiments, the lubrication film thickness in the observed points did not change much over time. The film thickness tended to stabilize at
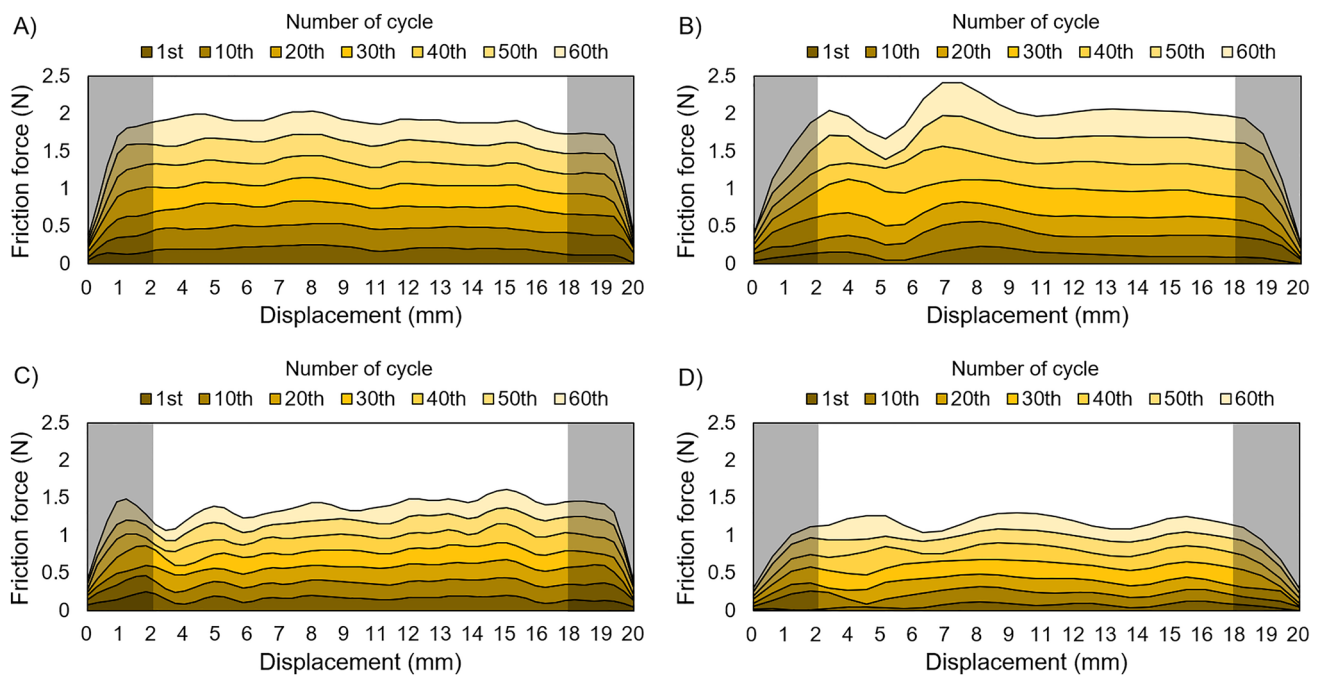
Fig. 8 Friction force development for Ti6Al4V **A** 20 mm/s, **B** 40 mm/s and CoCrMo, **C** 20 mm/s, **D** 40 mm/s

different values depending on the configuration: ~ 20 nm (CoCrMo), ~ 75 nm (Ti6Al4V) at 20 mm/s; and ~ 55 nm (CoCrMo), ~ 65 (Ti6Al4V) at 40 mm/s. As shown in the previous average values of film thicknesses, the Ti alloy reached overall higher values. These findings are related to the study of Ranuša et al. [20], where, in the experiments with Ti alloy, there were more adhered proteins in the contact area compared to the experiments with Co alloy. Therefore, we believe that a higher number of proteins in the contact area leads to an increase in lubrication film thickness. This statement is also supported by the study of Nečas et al. [15], where the development trends of film thickness measured by colorimetric interferometry were similar to the trends obtained by observing individual constituents in SF by fluorescent microscopy.

The behaviour of lubrication film formation with synovial fluid described by Myant et al. [39] showed the formation of aggregated proteins in the inlet zone. In the experiments performed in this study, the changes in the inlet zone, such as the formation of proteins, only occurred under specific conditions which appeared randomly. For example, the second pin from CoCrMo at 40 mm/s (see Fig. 5), where the film thickness increased significantly in the initial cycles until stabilizing at a similar value to other samples. After 10–30 cycles (depending on the observed point), the inlet zone disappeared (see Fig. 9), and the observed contact area behaved in the same way as in the other configurations. The reason, why the inlet zone appeared, was apparently due to the denser occurrence of proteins, which, however, were

moved away over time and the aforementioned stabilization occurred.

Although Protein Aggregation Lubrication (PAL) characteristics occurred, it was only under specific conditions (mentioned above) or at the beginning and end of the cycles, where the relative speed was very low and these values were not considered in the evaluation. Based on the observations, a higher number of proteins is needed to create characteristic PAL conditions. Nevertheless, the used model SF was prepared on the basis of the extracted samples from patients after arthroplasty [33], so the composition of the model SF should correspond to the real state of the human joints. Also, artificial starvation of the contact due to a lack of lubricant should not occur, as the contact pair was completely flooded. At the same time, the good flooding was checked during the experiments, and, if necessary, lubricant was added to prevent its occurrence. As can be seen from the pictures, while a visible inlet zone occurs, the film thickness is much higher (see Figs. 2, 4. PIN from CoCrMo). In order to improve the lubrication mechanism, an effort should be made to keep as many proteins as possible in the contact zone and its surroundings, which will lead to an increase in the overall thickness of the lubrication film.

Nissim et al. [40] created a computational model for PAL, which is typical for SF-lubricated contacts with. For the evaluation of the computational model, the results from Myant et al. [41] were used. The model showed quite a good compliance between experimental and simulation data. Furthermore, the model described the differences between PAL

Fig. 9 Creation of inlet zone (on the right side) with protein aggregation (marked with black dashed lines) for CoCrMo at 40 mm/s: **A** 5th cycle, **B** 15th cycle, **C** 25th cycle, **D** 30th cycle
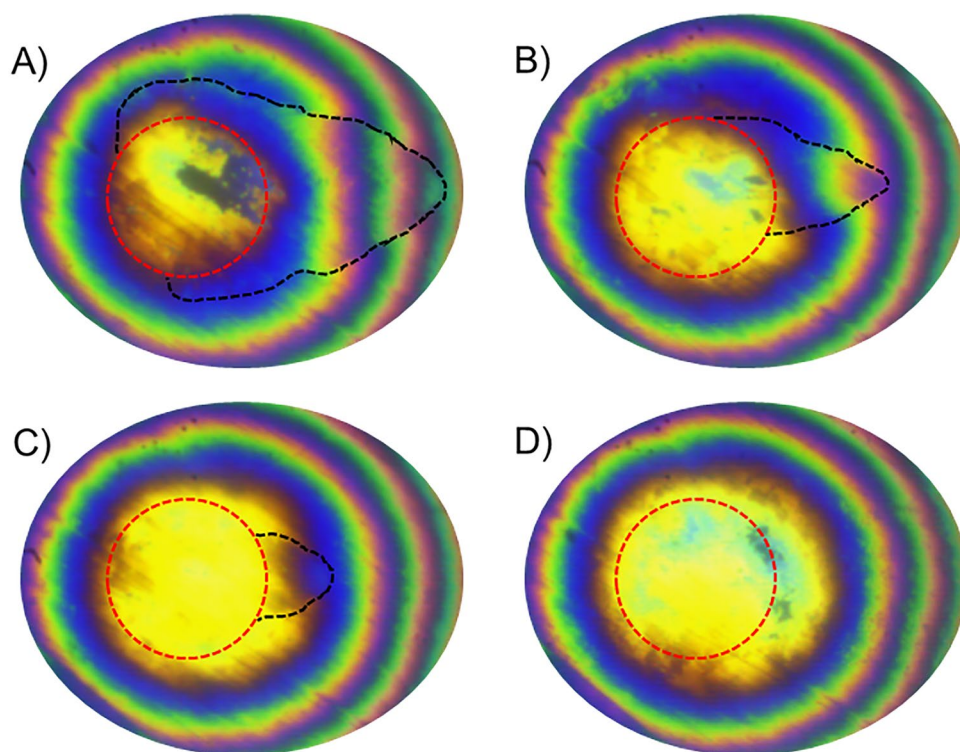
and EHL regimes and showed that the presented model for PAL is more in coincidence with experimental data. For the presented study, the obtained data do not fully correspond with the described model. The experimental results, such as the height of the lubrication film thickness did not reach such values as the model presents, but it also did not behave as a classic EHL regime. As both this study and the described simulation worked with the same contact pairs (CoCrMo on glass), it is possible to compare these results. For a steady lubrication film thickness, the values are as follows: 20 nm (EHL model), 140 nm (PAL model), and 40 nm (experiments in this study) for relative speed of 20 mm/s, and 30 nm (EHL model), 190 nm (PAL model), and 55 nm (experiments in this study) for relative speed of 40 mm/s. The main differences occur in the formation of aggregated proteins in the inlet zone, as the results in this study showed that the inlet zone was formed only in a few conditions, where the lubrication film thickness was much higher and could be comparable with the PAL model. As the conformity of the contact pair could play a major role in the ability to form stable inlet zones, this problem could have occurred due to the divergence in the radius of the tested or simulated pins. While a pin radius of 15 mm was used in this study, the PAL model used a radius of 19 mm. Moreover, the commonly used first MTP joint replacements have an even higher conformity (as the structure is comparable to THR–ball-in-socket), so it may be necessary to bring the experimental setup closer to reality to achieve more accurate results for this problem.

When trying to put together the knowledge of all the parameters measured or observed in this study, certain correlations can be found. The main findings were made for the CoCrMo configuration at 40 mm/s, which showed that it is possible to generate a sufficiently thick lubrication film to separate contact pairs, as this configuration did not show any wear scars on the tested pins. This fact is accompanied by the development of friction (see Fig. 7). This configuration showed the most unstable curve (see SD in Fig. 6), as well as the lowest values of friction compared to the other configurations. Moreover, the unloading phases at the 20 and 40 cycles showed a significant momentary decrease in CoF. On the other hand, the other configurations did not show such behaviour, and it can be said that these material combinations did not show good enough results at defined speeds. In order to obtain a good behaviour of the Ti alloy, certain adjustments of the contact surface have to be made.

In all the tested configurations, the CoF stabilized at the value of 0.4 (see Fig. 7). The only observable evolution occurred at the beginning of the experiments, where the CoF increased with sequent cycles. As well as materials, the change of relative speed did not visibly influence the CoF. This finding confirms that the contact pressure mainly affects the CoF by increasing the load for identical contact pairs [21, 22, 42] when the contact is under full-slip conditions, so that the slide-to-roll ratio does not enter this problem as a variable parameter. Although the force has changed slightly in the results presented due to different

material properties (0.5 N and 0.73 N), the contact pressure has remained the same.

4.1 Data Repeatability

The data repeatability in tribological problems using model synovial fluid as a lubricant could be more difficult to obtain due to its complex composition. To avoid this problem, the SF model used was prepared at one time, so the concentration of each constituent should be similar. Also, the tested samples could differ in their geometry or surface roughness. Each configuration was tested on three different contact pairs in order to obtain a sufficiently large set of results to provide sufficient repeatability. As shown in Figs. 3 and 4, the overall development of film thickness was similar for the different samples. Nevertheless, some differences can be found. For example, the lubrication film thickness is highly affected at the beginning of the experiment, or after each unloaded phase. Figures 3 and 4 show that proteins at different concentrations can enter the contact area after the application of load, which leads to a significant increase in lubrication film thickness (e.g. Pin 2 in CoCrMo at 40 mm/s). Although this increase occurs, the lubrication film thickness stabilizes after a few cycles at a value similar to other tested samples.

4.2 Limitations of the Study

The first MTP joint is very complex, and it is not easy to precisely describe its movement during the gait. Also, no ISO standard can be used to define the movement and later to compare different designs of experiments. In this study, the task was solved in a simplified configuration (pin-on-plate) in order to easily characterize the occurring phenomena. The kinematics and load were chosen based on the literature or tribometer capabilities. However, these input conditions do not fully correspond to reality as the conformity of the real pair was not considered. Another adjustment from the real joint was that the conventional contact pair was changed, as one component had to be transparent to enable the use of colorimetric interferometry. The glass plate was used as the transparent part. This glass plate has quite different material properties to those conventionally used in joint replacements. This change may have affected the ability of protein to be absorbed onto the contact pairs, as this phenomenon was identified as one of the main tribological problems with synovial fluid. While the glass was highly hydrophilic, the alloys were almost at the boundary between hydrophobic and hydrophilic behaviour. The values of the angle of wettability (AoW) are summarized in Table 4. Another difference arises in the dimensions of the contact area. The estimated contact areas for the configuration with glass are 0.095 mm for CoCrMo, respectively, 0.115 mm for Ti6Al4V. These values represent approximately 30% of the contact area obtained

Table 4 The angles of wettability for each material

Material	Angle of wettability	SD
CoCrMo	75.43°	1.65°
Ti6Al4V	78.21°	2.27°
Glass B270	29.08°	3.12°

in typical joint materials (CoCrMo and UHMWPE). However, if we consider the glass to represent a hard contact (as mentioned earlier), it would be better to compare the contact area with a metal-on-metal total joint replacement, where the contact areas will be practically comparable (0.112 mm for Ti6Al4V/Ti6Al4V and 0.115 mm for Ti6Al4V/Glass).

5 Conclusions

The complex friction, lubrication film formation, and wear scar analyses were obtained using a pin-on-plate configuration on a universal tribometer with colorimetric interferometry as the optical observation method. The experiments compared two human joint implant materials, conventional CoCrMo and Ti6Al4V that might find its use in the future for certain benefits (e.g. simplifying the joint geometry, and comparable material properties to bone) at two different relative speeds. The main conclusions, summed up in bullet points, are:

- Overall, the Ti alloys produced a thicker lubrication film than the Co alloys. Nevertheless, the thickness was not sufficient due to its inferior surface quality.
- The only tested configuration that created a lubrication film layer thick enough to separate the contact pair was the combination of CoCrMo with glass at a relative speed of 40 mm/s, where the signs of wear also did not occur.
- The described PAL, while using the SF model, was found only in specific conditions or at low speeds at the dead ends of the cycle. While protein aggregation occurred in the inlet zone, a thicker lubrication film was formed.
- The wear mechanism differs for CoCrMo and Ti6Al4V. The Co alloy is more likely to create the regular oval wear area. On the other hand, the Ti alloy creates bounded grooves that are significantly deeper.
- The values of friction were comparable for both tested alloys.

To sum up the results and answer the scientific questions mentioned in the introduction to this work. Certain differences were found in the lubrication mechanisms of tested alloys. The experiments with Ti6Al4V showed that this alloy can create a thicker lubrication film than a Co alloy. Nevertheless, it is necessary to mention the surface quality, or its

roughness. It was not possible to bring the quality of the surfaces close enough to each other by using conventional polishing methods due to the different material characteristics. This problem was observed with the Ti alloy where even a thicker film was not sufficient enough because the thickness of the lubricant did not overcome the average surface roughness, so that the contact pairs were not separated. To avoid this problem, it is necessary to improve the surface quality of Ti alloy. Two possible ways of achieving this are using non-conventional machining/polishing or applying surface coatings which in the past have shown a positive influence on the contact pair behaviour in various branches of tribology. The coating could also benefit the wear mechanism by decreasing the number of wear particles or reducing the depth of the grooves observed in this study. Another way of improving the tested tribological system could be surface texturing, which might bring the desired outcome, as it has been shown in the past that the textures can increase the film thickness.

Based on the findings of this study, it seems that the Ti6Al4V alloy may be suitable as a material for small joint implants. Nevertheless, it is not possible to use unmodified surfaces as the results of this tribological system are insufficient compared to the conventional CoCrMo alloy in terms of achieving a sufficiently thick lubrication film to separate the contact pair and thus prevent the undesirable wear of joint implants. Future studies should focus on describing the lubrication mechanism for additively manufactured Ti6Al4V with the aim of improving its behaviour by surface texturing and coating.

Declarations

References

1. Korim, M.T., Allen, P.E.: Effect of pathology on union of first metatarsophalangeal joint arthrodesis. Foot. Ankle. Int. **36**, 51–54 (2015). https://doi.org/10.1177/1071100714549046

2. França, G., Nunes, J., Pinho, P., Freitas, D., Andrade, R., Espregueira-Mendes, J., et al.: Is arthrodesis still the best treatment option for first metatarsophalangeal joint arthritis?—a systematic review of arthrodesis and arthroplasty outcomes. Ann. Jt. **6**, 5–5 (2021). https://doi.org/10.21037/aoj-20-88

3. Milstrey, A., Domnick, C., Garcia, P., Raschke, M.J., Evers, J., Ochman, S.: Trends in arthrodeses and total joint replacements in foot and ankle surgery in Germany during the past decade—back to the fusion? Foot. Ankle. Surg. **27**, 301–304 (2021). https://doi.org/10.1016/j.fas.2020.05.008

4. Titchener, A.G., Duncan, N.S., Rajan, R.A.: Outcome following first metatarsophalangeal joint replacement using TOEFIT-PLUS™: a mid term alert. Foot. Ankle. Surg. **21**, 119–124 (2015). https://doi.org/10.1016/j.fas.2014.10.005

5. Esway, J.E., Conti, S.F.: Joint replacement in the hallux metatarsophalangeal joint. Foot. Ankle. Clin. **10**, 97–115 (2005). https://doi.org/10.1016/j.fcl.2004.09.002

6. Narra, S.P., Mittwede, P.N., DeVincent, W.S., Urish, K.L.: Additive manufacturing in total joint arthroplasty. Orthop. Clin. North Am. **50**, 13–20 (2019). https://doi.org/10.1016/j.ocl.2018.08.009

7. Ni, J., Ling, H., Zhang, S., Wang, Z., Peng, Z., Benyshek, C., et al.: Three-dimensional printing of metals for biomedical applications. Mater. Today Bio. **3**, 100024 (2019). https://doi.org/10.1016/j.mtbio.2019.100024

8. Dreyer, M.J., Taylor, W.R., Wasmer, K., Imwinkelried, T., Heuberger, R., Weisse, B., et al.: Anomalous wear behavior of UHMWPE during sliding against CoCrMo under varying cross-shear and contact pressure. Tribol. Lett. **70**, 119 (2022). https://doi.org/10.1007/s11249-022-01660-w

9. Niinomi, M.: Mechanical biocompatibilities of titanium alloys for biomedical applications. J. Mech. Behav. Biomed. Mater. **1**, 30–42 (2008). https://doi.org/10.1016/j.jmbbm.2007.07.001

10. Ran, Q., Yang, W., Hu, Y., Shen, X., Yu, Y., Xiang, Y., et al.: Osteogenesis of 3D printed porous Ti6Al4V implants with different pore sizes. J. Mech. Behav. Biomed. Mater. **84**, 1–11 (2018). https://doi.org/10.1016/j.jmbbm.2018.04.010

11. Durrant, M., Durrant, L., McElroy, T.: Establishing a common instantaneous center of rotation for the metatarso-phalangeal and metatarso-sesamoid joints: a theoretical geometric model based on specific morphometrics. J. Orthop. Surg. Res. **14**, 107 (2019). https://doi.org/10.1186/s13018-019-1110-4

12. Flavin, R., Halpin, T., O'Sullivan, R., FitzPatrick, D., Ivankovic, A., Stephens, M.M.: A finite-element analysis study of the metatarsophalangeal joint of the hallux rigidus. J. Bone Joint Surg. Br. **90-B**, 1334–1340 (2008). https://doi.org/10.1302/0301-620X.90B10.20506

13. Al-Munajjed, A.A., Bischoff, J.E., Dharia, M.A., Telfer, S., Woodburn, J., Carbes, S.: Metatarsal loading during

gait—a musculoskeletal analysis. J. Biomech. Eng. **138**, 1–6 (2016). https://doi.org/10.1115/1.4032413

14. Myant, C., Underwood, R., Fan, J., Cann, P.M.: Lubrication of metal-on-metal hip joints: the effect of protein content and load on film formation and wear. J. Mech. Behav. Biomed. Mater. **6**, 30–40 (2012). https://doi.org/10.1016/j.jmbbm.2011.09.008

15. Nečas, D., Vrbka, M., Urban, F., Křupka, I., Hartl, M.: The effect of lubricant constituents on lubrication mechanisms in hip joint replacements. J. Mech. Behav. Biomed. Mater. **55**, 295–307 (2016). https://doi.org/10.1016/j.jmbbm.2015.11.006

16. Furmann, D., Nečas, D., Rebenda, D., Čípek, P., Vrbka, M., Křupka, I., et al.: The effect of synovial fluid composition, speed and load on frictional behaviour of articular cartilage. Materials (Basel) (2020). https://doi.org/10.3390/ma13061334

17. Nečas, D., Vrbka, M., Gallo, J., Křupka, I., Hartl, M.: On the observation of lubrication mechanisms within hip joint replacements. Part II: hard-on-hard bearing pairs. J. Mech. Behav. Biomed. Mater. **89**, 249–59 (2019). https://doi.org/10.1016/j.jmbbm.2018.09.026

18. Čípek, P., Vrbka, M., Rebenda, D., Nečas, D., Křupka, I.: Biotribology of synovial cartilage: role of albumin in adsorbed film formation. Eng. Sci. Technol. an Int. J. **34**, 101090 (2022). https://doi.org/10.1016/j.jestch.2021.101090

19. Nečas, D., Vrbka, M., Marian, M., Rothammer, B., Tremmel, S., Wartzack, S., et al.: Towards the understanding of lubrication mechanisms in total knee replacements – part I: experimental investigations. Tribol. Int. **156**, 106874 (2021). https://doi.org/10.1016/j.triboint.2021.106874

20. Ranuša, M., Čípek, P., Vrbka, M., Paloušek, D., Křupka, I., Hartl, M.: Tribological behaviour of 3D printed materials for small joint implants: a pilot study. J. Mech. Behav. Biomed. Mater. **132**, 105274 (2022). https://doi.org/10.1016/j.jmbbm.2022.105274

21. Nuño, N., Amabili, M., Groppetti, R., Rossi, A.: Static coefficient of friction between Ti-6Al-4V and PMMA for cemented hip and knee implants. J. Biomed. Mater. Res. **59**, 191–200 (2002). https://doi.org/10.1002/jbm.1233

22. Saikko, V.: Effect of contact pressure on wear and friction of ultra-high molecular weight polyethylene in multidirectional sliding. Proc. Inst. Mech. Eng. Part H J. Eng. Med. **220**, 723–731 (2006). https://doi.org/10.1243/09544119JEIM146

23. Gao, L., Hua, Z., Hewson, R., Andersen, M.S., Jin, Z.: Elasto-hydrodynamic lubrication and wear modelling of the knee joint replacements with surface topography. Biosurf. Biotribol. **4**, 18–23 (2018). https://doi.org/10.1049/bsbt.2017.0003

24. Flannery, M., Jones, E., Birkinshaw, C.: Analysis of wear and friction of total knee replacements part II: Friction and lubrication as a function of wear. Wear **265**, 1009–1016 (2008). https://doi.org/10.1016/j.wear.2008.02.023

25. Barceinas-Sanchez, J.D.O., Alvarez-Vera, M., Montoya-Santiyanes, L.A., Dominguez-Lopez, I., Garcia-Garcia, A.L.: The coefficient of friction of UHMWPE along an entire walking cycle using a ball-on-disc tribometer under arthrokinematics and loading conditions prescribed by ISO 14243–3:2014. J. Mech. Behav. Biomed. Mater. **65**, 274–280 (2017). https://doi.org/10.1016/j.jmbbm.2016.08.032

26. Shinmori, H., Kubota, M., Morita, T., Yamaguchi, T., Sawae, Y.: Effects of synovial fluid constituents on friction between UHMWPE and CoCrMo. Tribol ONLINE **15**, 283–292 (2020). https://doi.org/10.2474/trol.15.283

27. Guezmil, M., Bensalah, W., Mezlini, S.: Tribological behavior of UHMWPE against TiAl6V4 and CoCr28Mo alloys under dry and lubricated conditions. J. Mech. Behav. Biomed. Mater. **63**, 375–385 (2016). https://doi.org/10.1016/j.jmbbm.2016.07.002

28. Grosse, S., Haugland, H.K., Lilleng, P., Ellison, P., Hallan, G., Høl, P.J.: Wear particles and ions from cemented and uncemented titanium-based hip prostheses—a histological and chemical analysis of retrieval material. J. Biomed. Mater. Res. Part B Appl. Biomater. **103**, 709–717 (2015). https://doi.org/10.1002/jbm.b.33243

29. Connors, J.P., Stelzer, J.W., Garvin, P.M., Wellington, I.J., Solovyova, O.: The role of the innate immune system in wear debris-induced inflammatory peri-implant osteolysis in total joint arthroplasty. Bioengineering **9**, 764 (2022). https://doi.org/10.3390/bioengineering9120764

30. Čípek, P., Rebenda, D., Nečas, D., Vrbka, M., Křupka, I., Hartl, M.: Visualization of lubrication film in model of synovial joint. Tribol. Ind. **41**, 387–93 (2019). https://doi.org/10.24874/ti.2019.41.03.08

31. Hartl, M., Krupka, I., Poliscuk, R., Liska, M., Molimard, J., Querry, M., et al.: Thin film colorimetric interferometry. Tribol. Trans. **44**, 270–276 (2001). https://doi.org/10.1080/10402000108982458

32. ProSpon n.d. https://www.prospon.cz/.

33. Galandáková, A., Ulrichová, J., Langová, K., Hanáková, A., Vrbka, M., Hartl, M., et al.: Characteristics of synovial fluid required for optimization of lubrication fluid for biotribological experiments. J. Biomed. Mater. Res. Part B Appl. Biomater. **105**, 1422–1431 (2017). https://doi.org/10.1002/jbm.b.33663

34. ISO 14243-3. Implants for surgery — wear of total knee-joint prostheses: part 3: loading and displacement parameters for wear-testing machines with displacement control and corresponding environmental conditions for test. 2nd ed. Switzerland: (2014).

35. ISO 14242-1:2014/AMD 1:2018, Implants for surgery - wear of total hip-joint protheses - part 1: loading and displacement parameters for wear-testing machines and corresponding enviromental conditions for test (2018).

36. Allan, J.J., McClelland, J.A., Munteanu, S.E., Buldt, A.K., Landorf, K.B., Roddy, E., et al.: First metatarsophalangeal joint range of motion is associated with lower limb kinematics in individuals with first metatarsophalangeal joint osteoarthritis. J. Foot. Ankle Res. **13**, 33 (2020). https://doi.org/10.1186/s13047-020-00404-0

37. Joyce, T.J.: Examination of failed ex vivo metal-on-metal metatarsophalangeal prosthesis and comparison with theoretically determined lubrication regimes. Wear **263**, 1050–1054 (2007). https://doi.org/10.1016/j.wear.2006.11.045

38. Stokes, I.A., Hutton, W.C., Stott, J.R.: Forces acting on the metatarsals during normal walking. J. Anat. **129**, 579–590 (1979)

39. Myant, C., Cann, P.: On the matter of synovial fluid lubrication: implications for metal-on-metal hip tribology. J. Mech. Behav. Biomed. Mater. **34**, 338–348 (2014). https://doi.org/10.1016/j.jmbbm.2013.12.016

40. Nissim, L., Butt, H., Gao, L., Myant, C., Hewson, R.: Role of protein concentration on transient film thickness in synovial fluid lubricated joints. Biotribology **28**, 100191 (2021). https://doi.org/10.1016/j.biotri.2021.100191

41. Myant, C.W., Cann, P.: The effect of transient conditions on synovial fluid protein aggregation lubrication. J. Mech. Behav. Biomed. Mater. **34**, 349–357 (2014). https://doi.org/10.1016/j.jmbbm.2014.02.005

42. Ranuša, M., Wimmer, M.A., Fullam, S., Vrbka, M., Křupka, I.: Analysis of friction in total knee prosthesis during a standard gait cycle. Lubricants **9**, 36 (2021). https://doi.org/10.3390/lubricants9040036